Table 5 . Concentrations of REE in sandstones from Huangliu formation (in ppm).

Well	SN	Md/μm	La	Ce	Pr	Nd	Sm	Eu	Gd	Tb	Dy	Ho	Er	Tm	Yb	Lu	Y	SUM	LREE	HREE	LREE/HREE	δCe	δEu	(La/Yb)$_N$	(Gd/Yb)$_N$
	1	120 (vf)	41.35	77.82	9.11	33.99	6.26	1.20	5.25	0.89	4.76	0.94	2.69	0.41	2.50	0.36	25.19	212.71	169.72	17.80	9.53	0.97	0.64	11.15	1.69
	2	120 (vf)	36.98	71.17	8.37	31.33	5.74	1.10	4.96	0.81	4.43	0.89	2.46	0.37	2.21	0.32	22.66	193.78	154.69	16.43	9.42	0.97	0.63	11.29	1.81
	3	160 (f)	29.84	58.47	6.78	25.69	4.76	0.98	4.18	0.69	3.71	0.72	2.02	0.30	1.78	0.26	18.74	158.91	126.52	13.65	9.27	0.99	0.67	11.29	1.89
B-8	4	150 (f)	28.31	56.14	6.60	25.88	4.87	1.02	4.36	0.74	3.93	0.77	2.13	0.31	1.89	0.27	20.04	157.26	122.82	14.40	8.53	0.99	0.68	10.08	1.86
	5	150 (f)	28.90	56.11	6.62	25.21	4.45	0.92	4.00	0.66	3.52	0.69	1.92	0.29	1.73	0.26	17.91	153.18	122.21	13.06	9.36	0.98	0.67	11.24	1.86
	6	160 (f)	27.30	53.90	6.37	24.15	4.48	0.90	3.98	0.66	3.54	0.69	1.93	0.30	1.69	0.27	17.62	147.76	117.09	13.05	8.97	0.98	0.65	10.89	1.90
	7	180 (f)	38.18	74.92	8.66	32.32	5.90	1.02	4.97	0.78	4.12	0.80	2.29	0.36	2.11	0.30	20.96	197.69	161.00	15.73	10.23	0.99	0.57	12.19	1.90
	8	170 (f)	27.17	54.06	6.23	23.90	4.51	0.95	3.99	0.65	3.35	0.64	1.85	0.26	1.56	0.24	16.53	145.89	116.82	12.54	9.32	1.00	0.68	11.76	2.07
	9	180 (f)	27.59	58.86	6.27	23.93	4.61	0.79	4.32	0.72	4.04	0.83	2.45	0.41	2.60	0.41	25.17	163.00	122.05	15.78	7.73	1.08	0.54	7.15	1.34
	10	100 (vf)	28.70	56.96	6.91	26.25	4.78	0.91	4.26	0.68	3.67	0.76	2.03	0.30	1.83	0.27	18.62	156.93	124.51	13.80	9.02	0.97	0.62	10.58	1.88
	11	90 (vf)	29.53	58.02	6.96	26.54	4.92	0.95	4.13	0.67	3.65	0.72	2.00	0.30	1.69	0.26	18.16	158.50	126.92	13.42	9.46	0.97	0.65	11.79	1.97
	12	90 (vf)	31.51	59.88	7.19	26.96	4.94	0.98	4.30	0.70	3.64	0.75	2.04	0.32	1.87	0.29	18.68	164.04	131.46	13.89	9.46	0.96	0.65	11.38	1.86
	13	90 (vf)	36.58	69.38	8.25	31.09	5.51	1.06	4.67	0.74	4.05	0.80	2.26	0.34	2.00	0.29	20.44	187.44	151.87	15.13	10.03	0.96	0.64	12.36	1.89
	14	70 (vf)	77.28	146.47	16.81	61.99	10.99	1.56	9.05	1.40	7.31	1.52	4.02	0.62	3.85	0.57	37.73	381.16	315.09	28.34	11.12	0.98	0.48	13.55	1.90
A-2	15	70 (vf)	40.67	78.87	9.19	34.45	6.29	1.12	5.36	0.87	4.66	0.97	2.69	0.41	2.51	0.38	24.66	213.10	170.59	17.85	9.56	0.98	0.59	10.94	1.73
	16	100 (vf)	32.67	62.62	7.38	27.96	5.07	1.00	4.29	0.69	3.63	0.71	2.03	0.29	1.72	0.25	17.99	168.28	136.69	13.60	10.05	0.97	0.66	12.78	2.01
	17	80 (vf)	31.15	58.76	7.17	27.18	4.84	0.99	4.20	0.69	3.63	0.73	2.04	0.30	1.97	0.27	19.21	163.14	130.10	13.83	9.41	0.95	0.67	10.64	1.72
	18	80 (vf)	31.12	58.50	7.14	27.00	4.90	0.98	4.28	0.70	3.79	0.75	2.08	0.31	1.81	0.28	19.58	163.22	129.64	14.00	9.26	0.94	0.66	11.62	1.91
	19	80 (vf)	30.81	59.03	7.10	27.15	4.92	0.99	4.17	0.70	3.76	0.74	2.02	0.33	1.96	0.27	19.09	163.05	130.00	13.95	9.32	0.96	0.67	10.60	1.72
	20	80 (vf)	30.99	60.50	7.18	27.32	4.97	0.98	4.25	0.68	3.62	0.71	1.99	0.30	1.73	0.26	17.79	163.24	131.93	13.52	9.75	0.98	0.65	12.11	1.99
	21	100 (vf)	31.40	60.56	7.26	27.22	5.08	1.01	4.24	0.71	3.79	0.72	2.06	0.31	1.86	0.28	19.06	165.55	132.53	13.96	9.50	0.97	0.67	11.36	1.83
	22	80 (vf)	38.51	69.70	8.48	31.83	5.74	1.13	5.14	0.86	4.78	0.96	2.69	0.43	2.67	0.41	26.15	199.49	155.40	17.94	8.66	0.93	0.64	9.72	1.55
	23	80 (vf)	31.41	57.19	7.15	27.25	5.30	1.02	4.81	0.84	4.59	0.91	2.60	0.40	2.53	0.37	23.24	169.62	129.32	17.05	7.58	0.92	0.62	8.36	1.53
	24	80 (vf)	24.15	46.12	5.50	21.04	3.89	0.81	3.45	0.56	2.98	0.58	1.69	0.25	1.46	0.21	15.64	128.35	101.52	11.19	9.08	0.96	0.68	11.15	1.91
A-6	25	100 (vf)	36.05	61.28	7.89	29.54	5.46	1.04	4.68	0.84	4.51	0.87	2.58	0.43	2.47	0.38	23.11	181.12	141.27	16.74	8.44	0.87	0.63	9.85	1.53
	26	80 (vf)	30.22	56.66	6.83	25.82	4.67	1.00	4.10	0.68	3.62	0.71	2.00	0.29	1.76	0.26	18.01	156.63	125.20	13.42	9.33	0.95	0.70	11.55	1.88
	27	100 (vf)	27.38	52.71	6.28	23.84	4.24	0.91	3.89	0.61	3.28	0.64	1.83	0.28	1.75	0.25	16.83	144.72	115.36	12.53	9.21	0.97	0.69	10.54	1.79
	28	90 (vf)	29.46	56.54	6.73	25.44	4.67	0.96	3.97	0.65	3.61	0.70	1.94	0.30	1.79	0.26	18.11	155.13	123.79	13.23	9.36	0.97	0.68	11.12	1.79

Note: δEu (Eu/Eu*)= (Eu)$_N$/((Sm)$_N$*(Gd)$_N$)$^{1/2}$; δCe(Ce/Ce*)= (Ce)$_N$/((La)$_N$*(Pr)$_N$)$^{1/2}$, chondrite normalization values are from Henderson (1984). SN= sample number; M=mean grain size from thin section; f=fine-grained sandstone; vf=very fine-grained sandstone
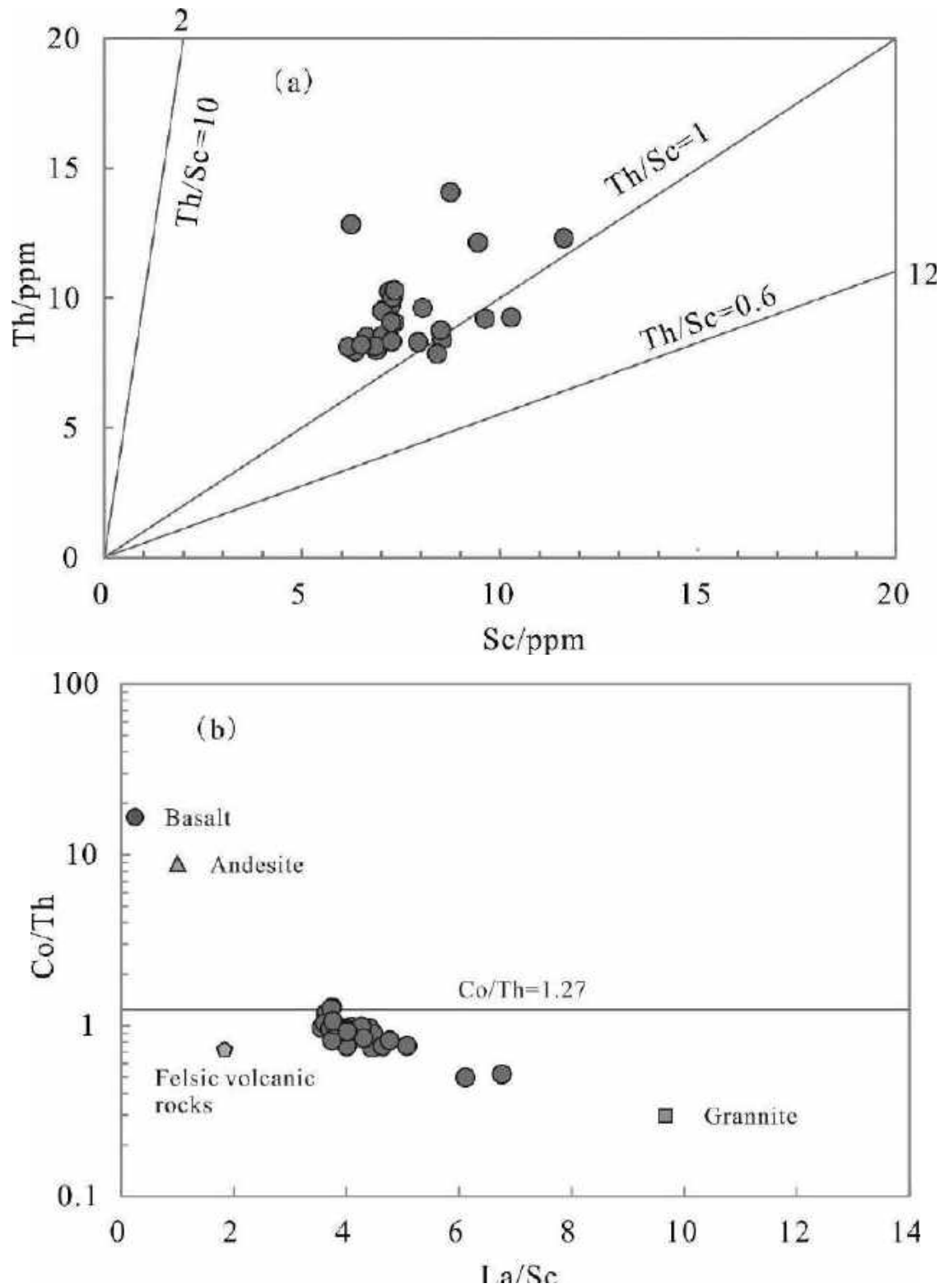
Fig. 8. (a) Th vs. -Sc and (b) Co/Th vs. -La/Sc for the analyzed sandstone (after Gu *et al*., 2002; Compositions for basalt, andesite, felsic volcanic rocks and granite are from Condie (1993)).

5. Discussion

5.1. Weathering and sediment maturity

The weathering of source rocks results in the removal and depletion of alkaline cations, such as Na^+, K^+, Ca^+, and the enrichment of Al_2O_3 (Nesbitt & Young, 1982). Therefore, the intensity of weathering can be evaluated by the amount of these elements (Nesbitt & Young, 1982). CIA is widely used to evaluate the intensity of weathering (Armstrong-Altrin, 2012; 2015; Zaid, 2013). CIA values >70 suggest a high intensity of chemical weathering. The CIA values of submarine fan sandstone indicate a moderate degree of chemical weathering in the source area. Furthermore, intensive chemical weathering often leads to an increase of Rb/Sr ratio (Nesbitt & Young, 1982), and high Rb/Sr (>1) indicates a high intensity of weathering (McLennan *et al*.,1993). The Rb/Sr values for submarine fan sandstone support the moderate chemical weathering (Table 4). The ratio of SiO_2/Al_2O_3 has also been widely used to evaluate the sediment maturity (Armstrong-Altrin, 2015; Zaid, 2013). SiO_2/Al_2O_3 >10 indicates high recycling and high chemical maturity. The SiO_2/Al_2O_3 ratios (average is 8.7) indicate moderate maturity. Fe_2O_3/K_2O and SiO_2/Al_2O_3 are also in accordance with litharenite, which is consistent with the petrological results (Fig. 6).

5.2. Source rock and provenance analysis

The sandstones derived from same source tend to have similar assemblages of heavy minerals (Morton, 2005; Fu *et al*., 2013). Though heavy minerals—especially the unstable heavy minerals—are relative easily affected by hydrodynamic conditions and alteration during diagenesis, the assemblage of heavy minerals is still useful in discriminating regional provenance (Morton, 2005; Fu *et al*., 2013). Therefore, neritic sandbar siltstone is sourced from Hainan Island when compared to the content of heavy minerals with that from Zhong *et al*. (2013). However, it is still difficult to differentiate between the source areas of the central Vietnam and Red River. Yet, Zhong *et al*. (2013) reported that the heavy mineral assemblages from the Dongfang area were similar to those of central Vietnam. The assumption was that both source rocks were complex, including different types of magmatic rocks and metamorphic rocks. Therfeore, it is necessary to combine other methods, such as geochemical data, to further confirm the provenance. The ratio of Al_2O_3/TiO_2 is considered to be one of the most functional provenance indicators of sedimentary rocks (Hayashi *et al*., 1997; El-Bialy, 2013). Hayashi *et al*. (1997) demonstrated that sandstone and mudstone have similar ratios to that of their source rocks. The positive correlation coefficient between Al_2O_3 and TiO_2 (Table 3) indicates insignificant fractionation of Al and Ti. The Al_2O_3/TiO_2 ratios (average is 14.5) of submarine fan sandstone indicate intermediate to felsic source rocks (Hayashi *et al*., 1997; El-Bialy, 2013).

REEs and several trace elements (e.g. Sc, Cr, Th, V, Ti, Hf, Zr) have been widely used in discriminating provenance due to their low mobility during weathering, sedimentation and diagenesis (Bhatia, 1983; Taylor *et al*., 1986; Taylor & McLennan, 1985; McLennan, 1989; McLennan *et al*., 1993; Schoenborn & Fedo, 2011). Mafic source rocks usually have low LREE/HREE ratios, whereas felsic source rocks usually have higher LREE/HREE ratios and a negative Eu anomaly. The REE patterns for all sandstone indicate a similar provenance. The LREE/HREE ratios (average is 9.3) and negative Eu anomaly (average is 0.64) indicate felsic source rocks (Rahman and Suzuki, 2007).

The ratios of trace elements (e.g. Th/Sc and Cr/Th) can provide useful information on the provenance of sedimentary rocks (Taylor & McLennan, 1985; Cullers & Berendsen, 1998; Feng & Kerrich, 1990; Cullers, 2000). The Co/Th and La/Sc ratios indicate felsic source rocks (Fig. 8b). The ratios of La/Sc, Th/Sc, Cr/Th and Eu/Eu* suggest that they are most likely derived from felsic source rocks (Armstrong-Altrin *et al*., 2004; Table 6).

Sandstone with a ratio of Cr/Ni>3 are significant in sedimentary fractionation (Garver *et al*., 1996). The content of Cr and Ni suggest that they are unlikely to be sourced from widespread mafic/ultramafic rocks. The Cr/Ni ratios of submarine fan sandstone indicate that they are more likely fractionated during weathering (Floyd *et al*., 1991; Zimmermann & Bahlburg, 2003; Rahman & Suzuki, 2007). Also, the high field strength elements (HFSEs) Zr and Hf, which tend to be more enriched in felsic rocks than mafic rocks (Feng & Kerrich, 1990; El-Bialy, 2013), are incompatible during most igneous processes. The content of Zr (average is 280ppm) is also supportive of felsic source rocks. However, the high content of Zr may be related to the reworking and sorting of sand during transportation from the Kutum uplift to the delta-front. Hf is closely related to Zr, and both elements are controlled by zircon.

The REE pattern of the studied rocks is similar to the upper Miocene sandstone sourced from central Vietnam (Shao *et al*., 2010; Cao *et al*., 2015) (Fig. 7b). Although there is no available REE data on the source rocks from central Vietnam, the felsic source rocks from the Kuntum uplift can provide the source material that was transported by the Blue River (Zhang *et al*., 2013; Zhong *et al*., 2013). The high Eu anomalies also may be due to felsic source rocks in the Kuntum uplift. In addition, recent offshore seismic profiling revealed eastward progradation from the Blue River to the

Yingxi slope of the Yinggehai Basin (Wang *et al*., 2015). The REE patterns are different to those of Red River sediment and Miocene sandstone sourced from Hainan Island (Clift *et al*., 2008; Zhao *et al*., 2013; Shao *et al*., 2010; Cao *et al*., 2015; Fig. 7). Also, heavy mineral assemblages of the submarine fan system differ from those of Hainan Island. Therefore, it is more likely that the Kuntum uplift provided the source material via the Blue River.

In addition, significant differences in quartz-feldspar-lithic fragments ratios were observed between the submarine fan and neritic sandbar systems. This finding indicates that the source rocks are the most important factor in determining the sandstone composition.

Table 6. Comparison of elemental ratio of sediment from Huangliu formation. Values for felsic and mafic sources are from Armstrong-Altrin *et al*., 2004 and upper continental crust is from Rudnick & Gao, 2003.

Elemental ratio	Huangliu Formation	Felsic sources	Mafic sources	Upper continental crust
La/Sc	3.56-6.76 (4.25*)	2.50-16.3	0.43-0.86	2.21
Th/Sc	0.90-2.25 (1.28*)	0.84-20.5	0.05-0.22	0.75
Cr/Th	3.23-7.03 (5.84*)	4.00-15.0	25.0-500	8.76
*Eu/Eu	0.48-0.70 (0.64*)	0.40-0.94	0.71-0.95	0.72

Note: * means average value.

5.3. Tectonic Setting and Significance of Provenance

Several trace elements (e.g. La, Th, Sc, Zr) have been widely used in discriminating tectonic settings due to their low mobility and well preserved source-rock information (Bhatia & Crook, 1986). The high La/Sc, Th/Sc and Zr/Sc are in accordance with a continental island arc origin (Fig. 9). However, Verma and Armstrong-Altrin (2013) and Armstrong-Altrin (2014) evaluated the trace-element diagrams proposed by Bhatia and Crook (1986) (Fig. 9) and cautioned that they may not work properly. Instead, Verma and Armstrong-Altrin (2013) proposed a new major-element based, multi-dimensional diagram with a better accuracy rate for tectonic discrimination of siliciclastic sediment. According to this diagram, most of the studied sandstones have a collision origin (Fig. 10). In general, this is in accordance with the continental island arc origin since it represents a convergent continental margin, just like a collision zone. It is also in agreement with transport from the Kuntum uplift because the South China Sea is located in the convergent hinge of the Eurasian, Pacific and Indo-Australian plates. The mountains in the Kuntum uplift were formed during Mesozoic Era by the collision between the Indochina Block and South China Block. At the end of the Paleocene, the Indochina Block moved southeastward as a result of collision between the Indosinian Plate and the Eurasian Plate. The northwest-trending faults in the border area exhibit left-lateral slip characteristics (e.g. Red River fault and Song Ma fault; Zhong *et al*., 2004; Sun *et al*., 2006). The amount of sediment from the Red River has decreased, and the sediment was replaced by estuarine deposits and coastal deposits when the Red River was captured by the Yangtze River at a time before the Oligocene (Zhao *et al*., 2013; Clark *et al*., 2004; Yan *et al*., 2011;). Zhao *et al*. (2013) reported that the sediment from the Red River was deposited only in the northwest part of the Yinggehai Basin from the late Oligocene to the Pleistocene. Instead, the Blue River in central Vietnam may have provided felsic material. Furthermore, the mouth of the Red River is mainly composed of argillaceous sediments, and less high-stand delta is developed (Wang, 1995).

The submarine fan sandstone sourced from the western Kuntum uplift is larger in grain size than the neritic sand bar siltstone. It is also rich in gas (Zhang *et al*., 2013) and beneficial in physical properties. This makes it a favorable exploration target. However, the neritic sandbar sourced from eastern Hainan Island has poor reservoir quality.
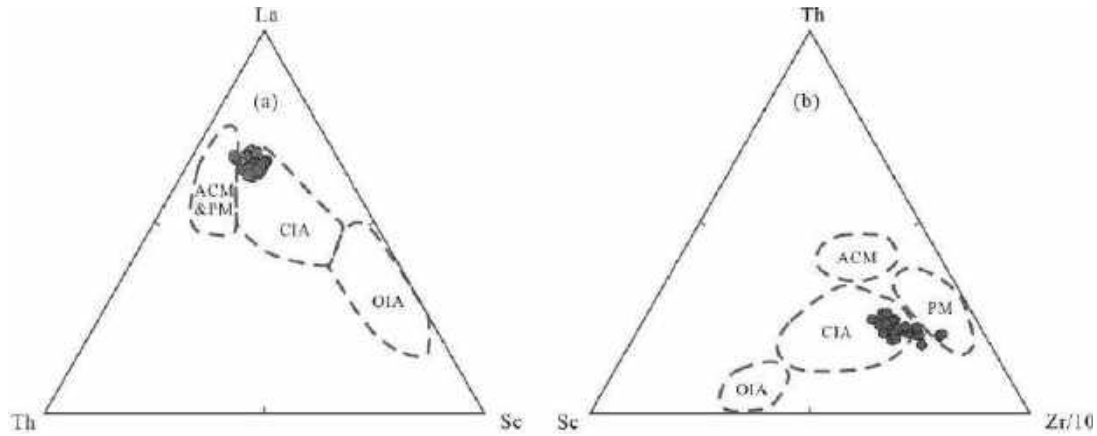
Fig. 9. Discrimination diagrams of tectonic setting for Huangliu formation using trace elements (after Bhatia & Crook, 1986). OIA = oceanic island arc; CIA = continental island arc; ACM = active continental margin; PM = passive margin.
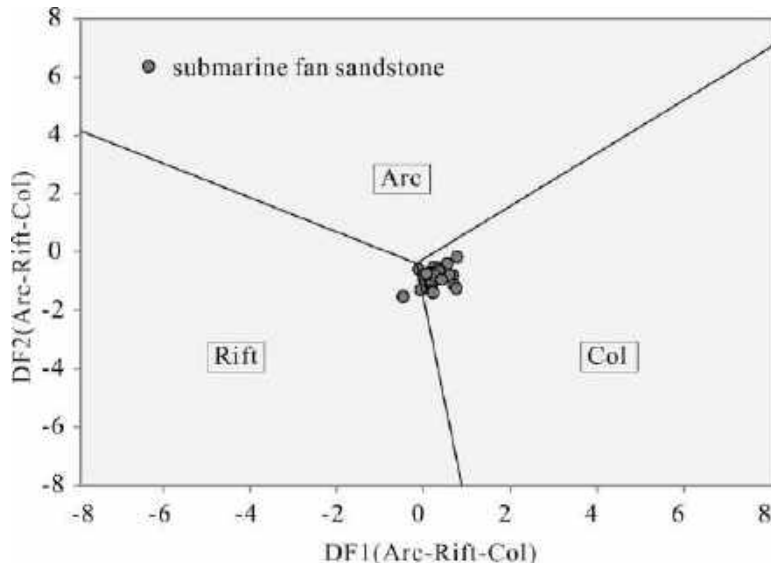
Fig. 10. Multidimensional discrimination diagrams of tectonic setting for the submarine fan sandstone (after Verma & Armstrong-Altrin, 2013). Arc = island or continental arc; Rift = continental rift; Col = collision).

$$DF1_{(Arc\text{-}Rift\text{-}Col)}= (-0.263\times\ln(TiO_2/SiO_2)_{adj})+ (0.604\times\ln(Al_2O_3/SiO_2)_{adj})+$$
$$(-1.725\times\ln(Fe_2O_3^t/SiO_2)_{adj})+ (0.660\times\ln(MnO/SiO_2)_{adj})+ (2.191\times\ln(MgO/SiO_2)_{adj})+$$
$$(0.144\times\ln(CaO/SiO_2)_{adj})+ (-1.304\times\ln(Na_2O/SiO_2)_{adj})+ (0.054\times\ln(K_2O/SiO_2)_{adj})+$$
$$(-0.330\times\ln(P_2O_5/SiO_2)_{adj})+1.588$$
$$DF2_{(Arc\text{-}Rift\text{-}Col)}= (-1.196\times\ln(TiO_2/SiO_2)_{adj})+ (1.064\times\ln(Al_2O_3/SiO_2)_{adj})+$$
$$(0.303\times\ln(Fe_2O_3^t/SiO_2)_{adj})+ (0.436\times\ln(MnO/SiO_2)_{adj})+ (0.838\times\ln(MgO/SiO_2)_{adj})+$$
$$(-0.407\times\ln(CaO/SiO_2)_{adj})+ (1.021\times\ln(Na_2O/SiO_2)_{adj})+ (-1.076\times\ln(K_2O/SiO_2)_{adj})+$$
$$(-0.126\times\ln(P_2O_5/SiO_2)_{adj})-1.068$$

6. Conclusions

This paper describes an integrated method to analyze the provenance of submarine fan sandstone. Petrography, heavy minerals assemblages, and geochemical compositions were used in this method. Based on the results of the investigation, the following conclusions can be drawn:

(1) Based on petrography, heavy mineral assemblages and geochemical composition, two provenances have been

identified. The submarine fan system and neritic sandbar are sourced from the Kuntum uplift and Hainan Island, respectively. Significant differences in quartz-feldspar-lithic fragments ratios and heavy mineral assemblages are observed from submarine fan and neritic sandbar system, which indicates that the source rocks are the most important factor in controlling the sandstone composition.

(2) The CIA values and Rb/Sr ratios of the submarine fan sandstones indicate moderate weathering intensity in the source

area. The values of SiO_2/Al_2O_3 indicate moderate sediment maturity. The REE patterns, diagrams and elemental ratios of trace elements of samples show that the submarine fan sandstones were derived from felsic source rocks. Finally, the results show that the integrated method used in this study is a powerful and effective tool in determining provenance when it is complex.

Acknowledgements

References

Akarish, A.I.M. & El-Gohary, A.M. (2008). Petrography and geochemistry of lower Paleozoic sandstones, East Sinai, Egypt: Implications for provenance and tectonic setting. Journal of African Earth Sciences, **52**(1), 43–54.

Armstrong-Altrin, J.S. (2015). Evaluation of two multidimensional discrimination diagrams from beach and deep-sea sediments from the Gulf of Mexico and their application to Precambrian clastic sedimentary rocks. International Geology Review, **57**(11-12): 1446-1461.

Armstrong-Altrin, J.S., Lee, Y.I., Kasper-Zubillaga, J.J., Carranza-Edwards, A., Garcia, D., Nelson Eby, G., Balaram, V. & Cruz-Ortiz, N.L. (2012). Geochemistry of beach sands along the western Gulf of Mexico, Mexico: Implication for provenance. Chemie der Erde **72**: 345–362.

Armstrong-Altrin, J.S., Lee, Y.I., Verma, S.P. & Ramasamy, S. (2004). Geochemistry of sandstones from the Upper Miocene Kudankulam Formation, southern India: Implications for provenance, weathering, and tectonic setting. Journal of Sedimentary Research, **74**(2): 285–297.

Armstrong-Altrin, J.S., Machain-Castillo M.L., Rosales-Hoz L, Carranza-Edwards A., Sanchez-Cabeza J.A. & Ruíz-Fernández, A.C. (2015). Provenance and depositional history of continental slope sediments in the southwestern Gulf of Mexico unraveled by geochemical analysis. Continental Shelf Research, **95**: 15-26.

Armstrong-Altrin, J.S., Nagarajan R., Lee Y.I., Kasper-Zubillaga J. & Córdoba-Saldaña L.P. (2014). Geochemistry of sands along the San Nicolás and San Carlos beaches, Gulf of California, Mexico: implications for provenance and tectonic setting. Turkish Journal of Earth Sciences, **23**: 533-558.

Bhatia, M.R. (1983). Plate tectonics and geochemical composition of sandstones. Journal of Geology, **91**(6): 611–627.

Bhatia, M.R. & Crook, K.A.W. (1986). Trace element characteristics of greywackes and tectonic setting discrimination of sedimentary basins. Contributions to Mineralogy and Petrology, **92**(2): 181–193.

Cao, L.C., Jiang, T., Wang, Z.F., Zhang, Y.Z. & Sun, H. (2015). Provenance of Upper Miocene sediments in the Yinggehai and Qiongdongnan basins, northwestern South China Sea: Evidence from REE, heavy minerals and zircon U-Pb ages. Marine Geology, **361**: 136-146.

Clark, M.K., Schoenbohm, L.M., Royden, L.H., Whipple, K.X., Burchfiel, B.C., Zhang, X., Tang, W., Wang, E. & Chen. L. (2004). Surface uplift, tectonics and erosion of Eastern Tibet from large-scale drainage patterns. Tectonics, **23**(1): 1–20.

Clift, P.D., Long, H.V., Hinton, R., Ellam, R.M., Hannigan, R., Tan, M.T., Blusztajn, J. & Duc, N.A. (2008). Evolving east Asian systems reconstructed by trace element and Pb and Nd isotope variations in modern and ancient Red River-Song Hong sediments. Geochemistry Geophysics Geosystems, **9**(4): 1-29.

Condie, K.C. (1993). Chemical composition and evolution of the upper continental crust: Contrasting results from surface samples and shales. Chemical Geology, **104**: 1–37.

Cullers, R.L. (2000). The geochemistry of shales, siltstones and sandstones of Pennsylvanian–Permian age, Colorado, USA: implications for provenance and metamorphic studies. Lithos, **51**: 181–203.

Cullers, R.L. & Berendsen, P. (1998). The provenance and chemical variation of sandstones associated with the Mid-continent Rift System, USA. European Journal of Mineralogy **10**(5): 987–1002.

Dickinson, W.R. (1985). Interpreting provenance relations from detrital modes of sandstones. In: Zuffa, G.G. (Ed.), Provenance of Arenites, NATO ASI Series 148, C: Mathematical and Physical Sciences. D. Reidel Publishing Co., Dordrecht-Boston, **148**: 333–361.

El-Bialy, M.Z. (2013). Geochemistry of the Neoproterozoic metasediments of Malhaq and Um Zariq formations, Kid metamorphic complex, Sinai, Egypt: Implications for source-area weathering, provenance, recycling, and depositional tectonic setting. Lithos, **175**–176: 63–85.

Feng, R. & Kerrich, R. (1990). Geochemistry of fine-grained clastic sediments in the Archean Abitibi greenstones belt, Canada: Implications for provenance and tectonic setting. Geochimica et Cosmochimica Acta, **54**(4): 1061–1081.

Floyd, P.A., Shail, R., Leveridge, B.E. & Franke, W. (1991). Geochemistry and provenance of Rhenohercynian synorogenic sandstones: Implications for tectonic environment discrimination. Geological Society, London, Special Publications, **57**(1): 173–188.

Folk, R.L. (1974). Petrology of Sedimentary Rocks. Hemphill, Austin, Texas, p. 182.

Fu, L., Guan, P., Zhao, W.Y, Wang M., Zhang, Y. & Lu, W.J. (2013). Heavy mineral feature and provenance analysis of Paleogene Lulehe Formation in Qaidam Basin. Acta Petrologica Sinica, **29**(8): 2867–2875 (in Chinese with English Abstract).

Garver, J.I., Royce, P.R. & Smick, T.A. (1996). Chromium and nickel in shale of the Taconic Foreland: A case study for the provenance of fine-grained sediments with an ultramafic source. Journal of Sedimentary Research, **66**(1): 100- 106.

Gu, X.X., Liu, J.M., Zheng, M.H., Tang, J.X. & Qi, L. (2002). Provenance and tectonic setting of the Proterozoic turbidites in Hunan South China: geochemical evidence. Journal of Sedimentary Research, **72**(3): 393 -407.

Hao, F., Dong, W.L., Zou, H.Y. & Yang, X.S. (2003). Overpressure fluid flow and rapid accumulation of natural gas in Yinggehai Basin. Acta Petrolei Sinica, **24**(6): 79- 85 (in Chinese with English Abstract).

Hayashi, K., Fujisawa, H., Holland, H.D. & Ohmoto, H. (1997). Geochemistry of 1.9 Ga sedimentary rocks from northeastern Labrador, Canada. Geochimica et Cosmochimica Acta, **61**(19): 4115–4137.

Henderson, P. (1984). Rare earth element geochemistry. Elsevier Amsterdam, p. 52- 71.

Herron, M.M. (1988). Geochemical classification of terrigenous sands and shales from core or log data. J. Sediment. Petrol., **58**(5): 820–829.

McLennan, S.M., Hemming, S., McDaniel, D.K. & Hanson, G.N. (1993). Geochemical approaches to sedimentation, provenance and tectonics. In: Johnson, M.J. & Basu, A. (Eds.), Processes Controlling the Composition of Clastic Sediments: The Geological Society of America, Special Paper, **285**: 21–40.

Moosavirad, S.M., Janardhana, M.R. & Sethumadhav, M.S. (2011). Geochemistry of lower Jurassic shales of the Shemshak Formation, Kerman Province, Central Iran: Provenance, source weathering, and tectonic setting. Chemie der Erde, **71**(3): 279–288.

Morton, A.C. (2005). Provenance of late Cretaceous to Paleocene submarine fan sandstones in the Norwegian Sea: Integration of heavy mineral, mineral chemical and zircon age data. Sedimentary Geology, **182**(1): 3–28.

Nesbitt, H.W. & Young, G.M. (1982). Early Proterozoic climates and plate motions inferred from major element chemistry of lutites. Nature, **299**: 715–717.

Nesbitt, H.W. & Young, G.M. (1996). Petrogenesis of sediment in the absence of chemical weathering: effects of abrasion and sorting on bulk composition and mineralogy. Sedimentology, **43**(2): 341–358.

Pei, J.X., Yu, J.F., Wang, L. F., Hao, D.F. & Liu, F. (2011). Key challenges and strategies for the success of natural gas exploration in mid-deep strata of the Yinggehai Basin. Acta Petrolei Sinica, **32**(4): 573–579 (in Chinese with English Abstract).

Pettijohn, F.J., Potter, P.E. & Siever, R. (1987). Sand and sandstone, 2nd ed. Springer-Verlag, New York. p. 553.

Rahman, M.J.J. & Suzuki, S. (2007). Geochemistry of sandstones from the Miocene Surma Group, Bengal Basin, Bangladesh: Implications for Provenance, tectonic setting and weathering. Geochemical Journal, **41**: 415–428.

Roser, B.P. & Korsch, R.J. (1988). Provenance signatures of sandstone–mudstone suites determined using discriminant function analysis of major-element data. Chemical Geology, **67**(1139–119 :(2-.

Saminpanya, S., Duangkrayom, J. & Jintasakul, P. (2014). Petrography, mineralogy and geochemistry of Cretaceous sediment samples from western Khorat Plateau, Thailand, and considerations on their provenance. Journal of Asian Earth Sciences, **83**: 13–34.

Schoenborn, W.A. & Fedo, C.M. (2011). Provenance and paleoweathering reconstruction of the Neoproterozoic Johnnie Formation, southeastern California. Chemical Geology, **285**: 231–255.

Shao, L., Li, A. & Wu, G.X. (2000). Evolution of sedimentary environment and provenance in Qiongdongnan Basin in the northern South China Sea. Acta Petrolei Sinica: **31**(4): 548552- (in Chinese with English Abstract).

Shen, S.Y., Wei, Q.R., Chen, H.L. & Mo, X.X. (1998). Tectonomagmatic types of volcanic rocks in Ailaoshan-Lixianjiang Belt, Nujiang River-Lanchangjiang River-Jinshajiang River area in China. Journal of Mineralogy and Petrology, **18**(2): 1824- (in Chinese with English Abstract).

Sun, M., Wang, H., Liao, J.H., Gan, H.J., Xiao, J., Ren, J.F. & Zhao, S.E. (2014). Sedimentary characteristics and model of gravity flow depositional system for the first member of Upper Miocene Huangliu Formation in Dongfang area, Yinggehai Basin, northwestern South China Sea. Journal of Earth Science, **25**(3): 506518-.

Sun, Z., Zhong, Z.H., Zhou, D., Xia, B., Qiu, X.L., Zeng, Z.X. & Jiang, J.Q. (2006). The development mechanism of the South China Sea. Science China: Earth Sciences, 36(9): 797–810 (in Chinese with English Abstract).

Taylor, S.R. & McLennan, S.H. (1985). The continental crust: Its composition and evolution. Blackwell Scientific Publications, Oxford, Melbourne. p. 312.

Taylor, S.R., Rudnick, R.L., McLennan, S.M. & Eriksson, K.A. (1986). Rare earth element patterns in Archean high-grade metasediments and their tectonic significance. Geochimica et Cosmochimica Acta, **50**(10): 2267–2279.

Verma, S.P. & Armstrong-Altrin, J.S. (2013). New multi-dimensional diagrams for tectonic discrimination of siliciclastic sediments and their application to Precambrian basins, Chemical Geology, **355**: 117–133.

Wang, H., Chen, S., Gan, H.J., Liao, J.H. & Sun, M. (2015). Accumulation mechanism of large shallow marine turbidite deposits: A case study of gravity flow deposits of the Huangliu Formation in Yinggehai Basin. Earth Science Frontiers, **22**(1): 21–34 (in Chinese with English Abstract).

Wang, P.X. (1995). ODP and Qinghai/Xizang (Tibetan) plateau. Advances in Earth Sciences, **10**(3): 254–257 (in Chinese with English Abstract).

Weltje, G.J. & Eynatten H.V. (2004). Quantitative provenance analysis of sediments: Review and outlook. Sedimentary Geology, **171**(1–4): 1–11.

Xie, Y.H., Zhang, Y.Z., Li, X.S., Zhu, J.C., Tong, C.X., Zhong, Z.H., Zhou, J.X. & He, S.L. (2012). Main controlling factors and formation models of natural gas reservoirs with high-temperature and overpressure in Yinggehai Basin. Acta Petrolei Sinica, **33**(4): 601–609 (in Chinese with English Abstract).

Yan, Y., Carter A., Palk C., Brichau S. & Hu X.Q. (2011). Understanding sedimentation in the Song Hong–Yinggehai Basin, South China Sea. Geochemistry Geophysics Geosystems, **12**(6).

McLennan, S.M. (1989). Rare earth elements in sedimentary rocks: influence of provenance and sedimentary processes. Mineralogical Society of America Reviews in Mineralogy, **21**(1): 169–200.

Zaid, S.M. (2013). Provenance, diagenesis, tectonic setting and reservoir quality of the sandstones of the Kareem Formation, Gulf of Suez, Egypt. Journal of African Earth Sciences, **85**: 31–52.

Zhang, H.L., Pei, J.X., Zhang, Y.Z., Jiang, C.Y., Zhu, J.C., Ai, N.P., Hu, Q.W. & Yu, J.F. (2013). Overpressure reservoirs of the Huangliu Formation of the Dongfang area, Yinggehai Basin, South China Sea. Petroleum Exploration and Development, **40**(3): 305–316 (in Chinese with English Abstract).

Zhang, Q.M. (1999). Evolution of Ying-Qiong Basin and its tectonic-thermal system. Natural Gas Industry, **19**(1): 12–17 (in Chinese with English Abstract).

Zhao, M., Shao, L., Liang, J.S., Qiao, P.J. & Xiang, X.H. (2013). REE character of sediment from the Paleo-Red River and its implication of provenance. Earth Science-Journal of China University of Geosciences, **38**(1): 61–69 (in Chinese with English Abstract).

Zhong, Z.H., Liu, J.H., Zhang, D.J., He, X.H., Zhang, Y.Z., Liu, X.Y., You, L. & Liu, X.Y. (2013). Origin and sedimentary characteristics of a large submarine fan in Dongfang area, Yinggehai Basin. Acta Petrolei Sinica, **34**(S2): 102–112 (in Chinese with English Abstract).

Zhong, Z.H., Wang L.S., Xia B., Dong, W.L., Sun, Z. & Shi, Y.S. (2004). The dynamics of Yinggehai Basin Formation and its tectonic significance. Natural Gas Industry, **78**(3): 302–309 (in Chinese with English Abstract).

Zimmermann, U. & Bahlburg, H. (2003). Provenance analysis and tectonic setting of the Ordovician clastic deposits in the southern Puna Basin, NW Argentina. Sedimentology, **50**(6): 1079–1104.

تحليل مصدر الحجر الرملي المترسب على مروحة غواصة في تشكيل هوانجليو، حقل غاز دونجفانج 13 في حوض ينج جيهاي، بحر الصين الجنوبي

ينتاو هوانج [1,2]، جوانكينج ياو [1,2]، فينجدي زهو [3]

[1] المختبر الرئيسي للتكتونيات والموارد البترولية (جامعة الصين للعلوم الجيولوجية)، وزارة التربية والتعليم، ووهان 430074، الصين

[2] كلية الموارد الأرضية، جامعة الصين للعلوم الجيولوجية، ووهان 430074، الصين

[3] كلية علوم الأرض، جامعة كوينزلاند، بريسبان QLD 4072، أستراليا

الملخص

يتكون الخزان الموجود في تشكيل هوانجليو الموسيني العلوي في حوض ينج جيهاي من رواسب على مروحة غواصة. يقدم هذا البحث طريقة متكاملة لتحليل المنشأ باستخدام البتروجرافية ونسبة تجمعات المعادن الثقيلة والتركيبات الجيوكيميائية. وتُظهر النتائج أن: (1) يوجد مصدرين، أحدهما في الغرب والآخر في الشرق. (2) يُظهر الحجر الرملي المترسب على مروحة الغواصة محتويات منخفضة من الزركون والتورمالين، ومحتويات عالية من المغنتيت والعقيق، في حين أن الصخور الرملية النتيرية تظهر خصائص معاكسة. (3) تشير قيم المؤشر الكيميائي للتغير (CIA) ونسب Rb / Sr للحجر الرملي على مروحة الغواصة إلى كثافة معتدلة التجوية في منطقة المنشأ. وتشير نسب مركب ثاني أكسيد السيلكون / أكسيد الألمونيوم SiO_2 / Al_2O_3 إلى وجود رواسب معتدلة. تشير أنماط $Th-La / Sc$، $Co / Th-Sc$ وREE إلى الانشقاق من صخور الصهارة الحمضية. (4) وتشير طريقة التكامل إلى أن الحجر الرملي على مروحة الغواصة مشتق غالبًا من رقعة KunTum الغربية. ونخلص في هذا البحث إلى أن دمج المركبات البترولية للحجر الرملي، وتجمعات المعادن الثقيلة والعناصر الرئيسية وعناصر الجيوكيمياء كلها عوامل مفيدة لتحديد هوية المصدر.